



OPEN

# Electronic hybridization detection in microarray format and DNA genotyping

SUBJECT AREAS:

BIOPHYSICS

BIOLOGICAL PHYSICS

Antoine Blin, Ismail Cissé &amp; Ulrich Bockelmann

Laboratoire Nanobiophysique ESPCI ParisTech, CNRS UMR Gulliver 7083 10 rue Vauquelin, 75005 Paris, France.

Received  
16 September 2013Accepted  
30 January 2014Published  
26 February 2014Correspondence and  
requests for materials  
should be addressed to  
U.B. (ulrich.  
bockelmann@espci.fr)

We describe an approach to substituting a fluorescence microarray with a surface made of an arrangement of electrolyte-gated field effect transistors. This was achieved using a dedicated blocking of non-specific interactions and comparing threshold voltage shifts of transistors exhibiting probe molecules of different base sequence. We apply the approach to detection of the 35delG mutation, which is related to non-syndromic deafness and is one of the most frequent mutations in humans. The process involves barcode sequences that are generated by Tas-PCR, a newly developed replication reaction using polymerase blocking. The barcodes are recognized by hybridization to surface attached probes and are directly detected by the semiconductor device.

The biological cell processes information by the specific interaction of biomolecules, while our society uses integrated semiconductor circuits for this purpose. A particularly direct way to bridge these worlds might thus consist in detecting specific binding of target molecules to a silicon device with embedded field effect transistors (FET). This principle was initially proposed forty years ago<sup>1</sup>. Together with the more recent use of integrated FET arrays, it generated two particularly exciting fields of applications to modern biology: neuroelectronic interfacing<sup>2</sup> and non-optical DNA sequencing<sup>3</sup>. DNA microarrays mostly rely on fluorescence, although FET-based detection of hybridization could provide advantages. Devices for FET readout could be simpler and smaller than fluorescence scanners. Moreover, the direct electronic detection could avoid errors caused by the use of fluorescence, as for instance inhomogeneous labelling efficiencies and photobleaching varying with ozone concentration<sup>4,5</sup>. Alternative detection schemes based on non-fluorescent labels exist. These labels however also have their specific disadvantages. Therefore, the label-free FET-based hybridization detection, which is based on direct detection of the intrinsic charge of the DNA molecule, has been studied by several groups<sup>6–13</sup>. What new elements could pave the way to a first application in the microarray field? Reproducibility is mandatory, but most prior publications present individual measurements. Use of micro-spots is required for the parallel detection with microarrays, but has not been shown in combination with direct FET-based hybridization detection so far. A definite biological application, ideally going from biological sample to medical relevant data in numerical format, has not yet been presented, but is needed to convince that all important technical criteria can be met.

Here we suggest genotyping of DNA mutations as an application of direct FET-based hybridization detection to the microarray field. Using electrolyte gated arrays, threshold voltage shifts of transistors exhibiting probe molecules of different base sequences are compared. A dedicated blocking procedure is presented that now allows using micro-spots. The process involves barcode sequences that are generated by Tas-PCR, a newly developed replication reaction using polymerase blocking. The barcodes are recognized by hybridization to surface attached probes and directly detected by the semiconductor device.

## Results

**Electronic detection of DNA oligonucleotide hybridization.** In the work presented in the main text of this article, we used two different probe sequences P1 and P2 (Ref. 14; see Table S3) and performed electronic measurements and hybridizations in 25 mM KCl at room temperature. A schematic view of the measurement configuration and an FET array with two micro-spots are shown in Fig. 1. Electronic detection of hybridization is illustrated in Fig. 2. In this case, probes P1 were spotted on transistors 7–16 and 53–61 and probes P2 on 31–41 and 77–88, followed by a two-step blocking procedure (see methods). Subsequent to this blocking the surface of the FET array was covered by a 1 mL volume of the 25 mM KCl solution and a first electronic measurement was performed. The voltages  $U_{SE}^i$  of all transistors are derived from this measurement (see methods). Then target oligonucleotides T2, complementary to P2, were added to obtain a final target concentration of 100 nM. After 10 min, this hybridization was stopped by rinsing with KCl, before a second measurement was performed, from

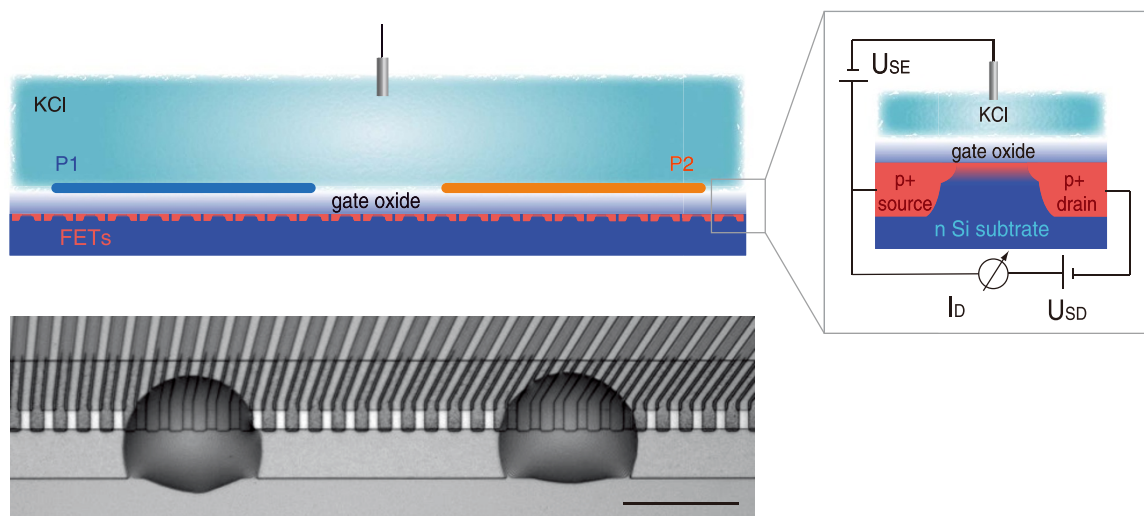


**Figure 1 | The FET array and its measurement configuration.** Top. Schematic cross-sectional view of an FET array with two regions where probes are attached to the oxide surface. Each probe region (P1 and P2) extends over several individual transistors (presented in red underneath the gate oxide). The surface of the device is covered by a KCl solution and a Ag/AgCl electrode is immersed. On the right, a zoom of an individual transistor with a schema of its electrical connections is presented. A voltage  $U_{SE}$  is applied between the electrode and a common source contact and a voltage  $U_{SD}$  is applied between the source contact and each individually connected drain. The drain currents  $I_D$  of all transistors are measured. Bottom. Microscope image of two microspots on a FET array. Each spot exhibits a diameter of approximately  $100 \mu\text{m}$  and covers about 5 individual transistors. The active (metal-free gate) regions appear as white rectangles. In the upper part, the light gray lines are individual drain connexions and the dark gray regions correspond to lateral electrical isolation. The wide rectangle in the middle corresponds to the region where a 500 nm thick oxide coating has been removed to expose the FET array to the electrolyte. The homogenous part in the bottom is the common source connexion. A  $100 \mu\text{m}$  scale bar is shown in the bottom right corner.

which the voltages ( $U_{SE}^f$ ) were derived. The first measurement of the array is thus performed before the hybridization, while the second measurement is performed afterwards. In Fig. 2, the difference  $\Delta U_{SE} = U_{SE}^f - U_{SE}^i$  between the two measurements is plotted for each FET of the array. Regions with DNA probes appear as distinct peaks, each extending over 9–12 FETs. We denote the average of the voltage differences  $\Delta U_{SE}$  measured by the FETs that carry probe P1 by  $\Delta U_{P1}$  and the average  $\Delta U_{SE}$  measured by the FETs that carry probe P2 by  $\Delta U_{P2}$ . From Fig. 2, we directly see that  $\Delta U_{P1} \sim$

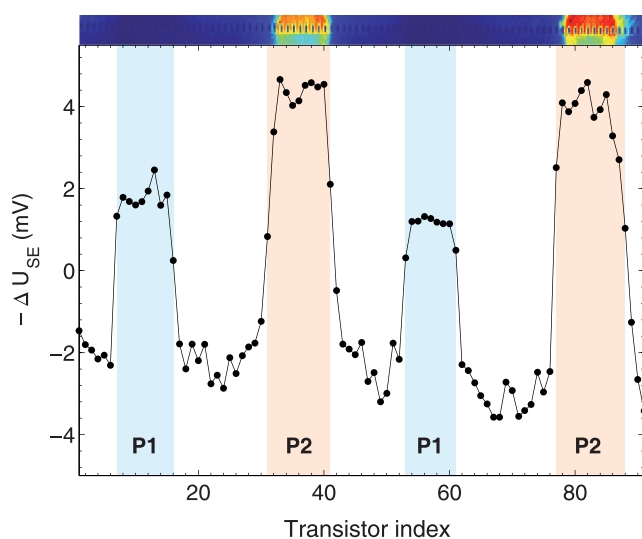


**Figure 2 | Electronic detection of DNA oligonucleotide hybridization.** Electronic detection of specific hybridization between P2 probe DNA and T2 target oligonucleotides is shown in the main figure. The image shown at the top visualizes the fluorescence signal arising from the hybridized Cy3-modified T2 targets. The individual transistors of the array are seen in the fluorescence image.

$-1.3 \text{ mV}$  and  $\Delta U_{P2} \sim -3.7 \text{ mV}$ . We then define the difference between the two average shifts  $\Delta U_{P1,P2} = \Delta U_{P1} - \Delta U_{P2}$  and obtain  $\Delta U_{P1,P2} \sim 2.3 \text{ mV}$ . As we will show below, this quantity  $\Delta U_{P1,P2}$  represents a reliable electronic signal of hybridization. After the electronic measurements, the sample was dried with air and a microscopic fluorescence image of the FET array was acquired using a custom microfluorescence setup<sup>15</sup>. For the image presented at the top of Fig. 2, the Cy3-labeled T2 target oligonucleotides were scanned under 532 nm laser excitation. The image shows fluorescence signal on the regions where P2 probes were spotted, but no corresponding signal for the P1 probes. The fluorescence measurement thus confirms that hybridization occurred specifically on probes P2.

Results of eight electronic hybridization measurements with four different FET arrays are compiled in Table 1. In each case we used multiple spots of P1 and P2 and performed hybridization either with target T1 or with target T2. An average shift of 2.3 mV is observed between the P1 and P2 regions. The sign of the shift reflects the direction of the hybridization: we observe that the transistors with DNA probes that are subject to hybridization exhibit smaller  $\Delta U_{SE}$  than the transistors with probes that do not hybridize. This is equivalent to the fact that the average  $\Delta U_{P1,P2}$ , shown in Table 1, is always negative for hybridization with target T1, while it is always positive for hybridization with T2. The sign of the average  $\Delta U_{P1,P2}$  thus characterizes DNA hybridization. It is similar in sign and magnitude to results of earlier DNA hybridization studies that involved field effect measurements with Si/SiO<sub>2</sub> structures and PLL mediated immobilisation of DNA oligonucleotide probes<sup>7,12</sup>. However, since in the earlier work no blocking procedure was used, the molecular layer was different and there was a significant amount of non-specific adsorption. The sign of the shift is in agreement with a common simplifying picture that DNA hybridization modifies the surface potential by adding the negative charges of the DNA target molecules. We found that a blocking procedure is required for electronic detection of DNA hybridization in microarray format.

The statistical analysis indicates that hybridization detection schemes based on only one probe DNA sequence are not robust.



Table 1 | Statistics of the electronic hybridization detection

Exp	target	$\Delta U_{P1}$	$\Delta U_{P2}$	$\Delta U_{P1,P2}$	Ok (abs,rel)	$\Delta U_{P1,PLL}$	$\Delta U_{P2,PLL}$
1a	T1	$4.6 \pm 0.5$	$6.7 \pm 0.3$	$-2.0 \pm 0.5$	47, 100	$-1.0 \pm 0.5$	$0.9 \pm 0.3$
1b	T2	$2.0 \pm 0.7$	$-0.4 \pm 0.4$	$2.4 \pm 0.7$	41, 100	$1.4 \pm 0.7$	$-1.0 \pm 0.4$
2a	T1	$-8.1 \pm 1.1$	$-3.7 \pm 0.8$	$-4.4 \pm 1.2$	29, 100	$-0.4 \pm 1.2$	$4.0 \pm 0.9$
2b	T2	$3.5 \pm 1.2$	$2.8 \pm 0.8$	$0.7 \pm 1.2$	16, 57	$-0.7 \pm 1.2$	$-1.4 \pm 0.8$
3a	T1	$8.2 \pm 0.3$	$10.3 \pm 0.6$	$-2.1 \pm 0.6$	19, 100	$-1.9 \pm 0.6$	$0.2 \pm 0.6$
3b	T2	$-1.3 \pm 0.3$	$-3.7 \pm 0.6$	$2.3 \pm 0.6$	21, 91	$-3.7 \pm 0.3$	$-6.0 \pm 0.6$
4a	T2	$1.8 \pm 0.4$	$-0.3 \pm 0.2$	$2.1 \pm 0.4$	18, 100	$0.1 \pm 0.4$	$-2.0 \pm 0.3$
4b	T1	$-5.5 \pm 0.4$	$-2.8 \pm 0.2$	$-2.6 \pm 0.4$	14, 100	$-1.6 \pm 0.4$	$1.0 \pm 0.3$

Two successive hybridizations were performed on each of four different FET arrays, without stripping surface bound DNA after the first hybridization. The leftmost column gives the number of the array and a suffix. Suffix a stands for the first hybridization, b for the second one. Either T1 or T2 target oligonucleotides were used, as given in the "target" column. Columns  $\Delta U_{P1}$  and  $\Delta U_{P2}$  display average and mean-square deviation of the threshold voltage shifts of the transistors covered by probes P1 and P2, respectively. Column  $\Delta U_{P1,P2}$  gives the difference  $\Delta U_{P1,P2} = \Delta U_{P1} - \Delta U_{P2}$ . We observe that the sign of the average  $\Delta U_{P1,P2}$  is always negative for hybridization with target T1 and always positive for hybridization with T2. This sign is thus interpreted as the electronic signal of specific hybridization. Number and percentage of individual FETs displaying the correct sign of the shift are provided by the "Ok" column. To derive this column, the difference between the  $\Delta U$  of each individual FET carrying probes complementary to the target DNA and the average shift of all transistors carrying the non-complementary probe DNA is calculated. It can be seen that the direction of specific hybridization is correctly detected by more than 90% of the FETs in seven out of eight recognition reactions. In total, 205 of 219 (94%) individual FET signals show the correct sign. We define  $\Delta U_{PLL}$  as the threshold voltage shift of the transistors without DNA probes. Columns  $\Delta U_{P1,PLL}$  and  $\Delta U_{P2,PLL}$  provide the difference  $\Delta U_{P1} - \Delta U_{PLL}$  and  $\Delta U_{P2} - \Delta U_{PLL}$ , respectively. Experiment 3b is presented in Fig. 2.

This can be seen by comparing the "target" column of Table 1 with any of the four columns  $\Delta U_{P1}$ ,  $\Delta U_{P2}$ ,  $\Delta U_{P1,PLL}$  or  $\Delta U_{P2,PLL}$ . Convincing correlation is not achieved. In contrast, when the average difference  $\Delta U_{P1,P2}$  between the transistors carrying probes P1 and P2 is used, reliable electronic detection of hybridization is obtained in all experiments. This robustness is based on the fact that the mode of hybridization detection used in this work is quite reliable even at the level of the individual transistors: as explained in the table caption, 205 out of 219 FETs showed a signal in agreement with the aforementioned expectation for specific hybridization. A FET array can be cleaned after hybridization detection as described in Methods and subsequently reused for a new round of probe immobilization and hybridization detection. Experiments 1a and 1b have been performed with a recycled array.

To analyze the quality of the spotted microarrays, we investigated the hybridization signals by fluorescence, using a commercial scanner with a spatial resolution of 3  $\mu\text{m}$ , see section 7 of the supplementary materials<sup>14</sup>. Overall, the arrays show performances that are typical of spotted fluorescence DNA microarrays. The spots are rather uniform in size, but still show some intra-spot and inter-spot variations in intensity. By reducing these variations it might thus be possible to improve the electronic detection of hybridization presented in this work.

**Tas-PCR and 35delG mutation genotyping.** As an application of the direct hybridization detection, we designed an assay for genotyping 35delG mutation, one of the most frequent mutations of the human genome. This deletion of one in a stretch of six guanines, occurs in gene GJB2 coding for the connexin-26 protein and is related to prelingual non-syndromic deafness<sup>16</sup>.

We have developed a new enzymatic replication reaction, called tagged allele-specific polymerase chain reaction or Tas-PCR. A detailed description is provided in the supplementary material<sup>14</sup>. Tas-PCR involves forward primers consisting of three blocks. These primers exhibit at their 5' end a sequence of 20 bases for specific recognition by hybridization (tag) and their 3' ends contain a sequence to prime PCR with the last two nucleotides assuring allele discrimination. These two sequences are linked by a short succession of carbon atoms (C18 spacer). If the template contains the wild type (wt) sequence, a 197 base pair double-stranded DNA molecule (ds-DNA) is synthesized with a 5' single stranded overhang of base sequence T2, as illustrated in Fig. 3a. The C18 spacer blocks the polymerase during PCR and ensures that the T2 sequence remains single-stranded. The single stranded overhang acts as a molecular barcode in subsequent molecular sorting by hybridization. If the template contains the mutation, ds-DNA with a barcode of sequence T1 is obtained (see Fig. 3b). For a heterozygote genotype, both wt and

mutated sequences are present. Our single tube duplex Tas-PCR would detect them in parallel, i.e. the product would contain both PCR fragments with T1 tag and fragments with T2 tag (see Fig. 3c). Electronic detection of T1 and T2 is subsequently performed by hybridization on a FET array with P1 and P2 spotted on different regions.

Genomic DNA extracted from patient blood was pre-amplified by PCR. We subject a small amount of the purified product to Tas-PCR<sup>14</sup> and perform hybridization of the purified product on a FET array. Slower hybridization kinetics was observed for Tas-PCR products than for oligonucleotide targets and therefore hybridization time and target concentration were increased to 3 hours and 800 nM, respectively. Otherwise, array preparation, probe immobilization, hybridization and detection procedures were as described above. Electronic and fluorescence measurements show specific hybridization on P1 probes, see Fig. 4. This means that only products with T1 barcode were generated and in turn that the substrate contained the mutated sequence and no wt sequence. Indeed, here we used a sample of genomic DNA that exhibits the 35delG mutation on both copies of the chromosome. It has been verified independently by DNA sequencing that the corresponding patient was a 35delG homozygote.

## Discussion

The amplitude of the threshold voltage shift observed between P1 and P2 for Tas-PCR fragments is comparable to the one observed for oligonucleotide targets. The shift thus does not simply reflect the total molecular charge of the target molecule. Screening of molecular charge by mobile ions should be taken into account. At 25 mM monovalent salt, the Debye screening length  $\lambda_D$  is about 2 nm, which makes the field effect detection surface selective. As the persistence length of ds-DNA ( $\sim 50$  nm) strongly exceeds  $\lambda_D$  it is thus conceivable that a significant fraction of a long ds-DNA target does not contribute to the electronic signal. Moreover, the molecular conformation of the PLL/DNA polyelectrolyte on the negatively charged SiO<sub>2</sub> surface is not known and both hybridization and change in salt concentration can induce conformational changes that are difficult to predict theoretically. Earlier experimental studies showed that single and double-stranded DNA of various lengths can be detected by the field effect transistor approach<sup>15</sup>. In this work we use 20-base barcode sequences. This is the typical length used in barcoding (or molecular tagging) strategies with DNA microarrays that can involve many thousand distinct barcodes<sup>17,18</sup>.

As described in supplementary materials<sup>14</sup>, section II, reduction of salt concentration to 10  $\mu\text{M}$  ( $\lambda_D \sim 100$  nm) in the electronic measurement, while keeping hybridization at 25 mM, enhanced the electronic signal of hybridization by about a factor of two. This increase

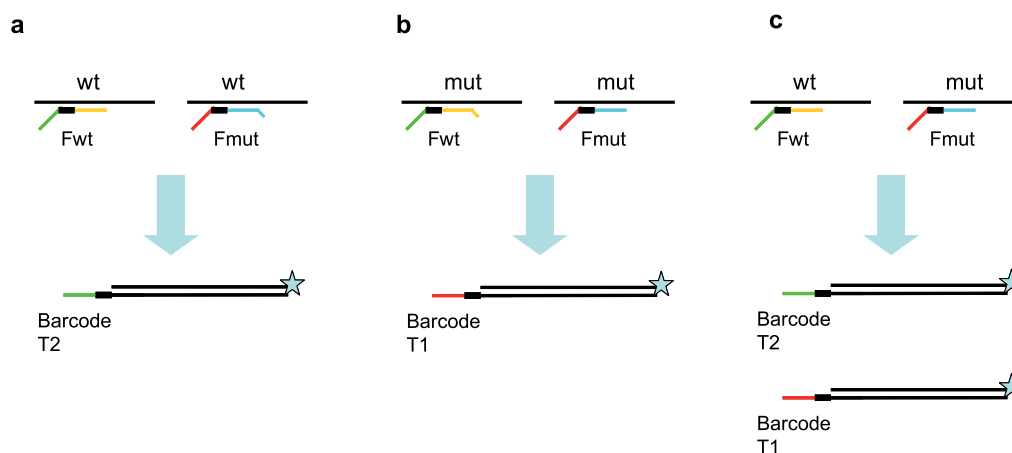


**Figure 3 | Principle of Tas-PCR genotyping.** (a) Homozygote wt sample. Forward primer Fwt is hybridized at its 3' end, while primer Fmut is mismatched. After Tas-PCR only molecules with barcode T2 are generated. (b) Homozygote mutant sample. Fmut is hybridized, while Fwt is mismatched. After Tas-PCR only molecules with barcode T1 are generated. (c) Heterozygote sample. Both Fwt and Fmut are hybridized. Tas-PCR generates molecules with barcodes T1 and T2.

in signal however did not lead to an improved reliability of the detection, because an increased variability of  $\Delta U_{P1,P2}$  was observed. The latter is tentatively attributed to the solution changes that are required when hybridization and detection are not performed at the same salt concentration. This suggests that automatization of the rinsing steps might help to reduce these variations. It remains that even for detection at 10  $\mu\text{M}$ , the present experiments gave correct hybridization detection, with a majority (86%) of individual FETs displaying expected signal and that genotyping of the 35 delG mutation was possible as well<sup>14</sup>.

The electronic detection of DNA hybridization used in this work measures the change of interface potential induced by the intrinsic charge of the target molecules. This approach has specific constraints. (i) Rather low salt concentrations (typically below 50 mM monovalent salt) have to be used during the measurement in order to

keep electrostatic screening sufficiently small, and in this case specific hybridization is more difficult to achieve than in the high salt regime commonly used with microarrays. (ii) The dynamic range of the electronic measurement is with two orders of magnitude<sup>19</sup> significantly smaller than the range of fluorescence measurements that reaches 3–4 decades. (iii) This label-free technique is not only sensitive to hybridization, but to other effects like non-specific adsorption of molecular species and changes in salt and pH. These effects can induce variation of the electrostatic potential at the solid/electrolyte interface by acting on the gate insulator and/or the molecular coating. (iv) Temporal drift of the FET threshold voltage sometimes amounts to the order of mV/min, which for a hybridization duration of 10 min or more can lead to voltage shifts that are comparable to the hybridization signal<sup>20</sup>.

The present results suggest that for the specific application of DNA genotyping these challenges could be met. Only a single patent was measured in this work. To demonstrate that the presented combination of tas-PCR and FET-based detection is a suitable genotyping approach, additional measurements with more patient samples, including the different genotypes (homozygote normal, heterozygote and homozygote mutated), are required. This will be subject of future work.

By genotyping DNA, we have deliberately chosen a case where the biological information exhibits a discrete character, a binary signal coded by presence or absence of a mutation at a given position in the DNA base sequence. In this case a dynamic range of two decades is fine. The situation is different for microarray analysis of gene expression, where expression levels are distributed continuously and can vary by more than three orders of magnitude. Also, in our case the molecular biology protocol applied before the hybridization generates a sample that contains DNA of appropriate concentration in low salt and is purified from other reagents that could perturb the electronic hybridization signals. The question about the utility of FETs as direct hybridization sensors for DNA microarray assays in general is beyond the scope of this work.

We find that two concepts are of particular importance for achieving reliable detection. The first is the differential measurement, where hybridization signals are derived from the comparison of voltage shifts measured on probes of different sequences. It circumvents aforementioned challenges iii and iv. The results compiled in table 1 show that for our measurements this concept is required to achieve reproducibility. The second concept is the Tas-PCR. It responds to issues related to challenges i and ii. Tas-PCR is the only allele-specific amplification that gives a homogenous set of DNA

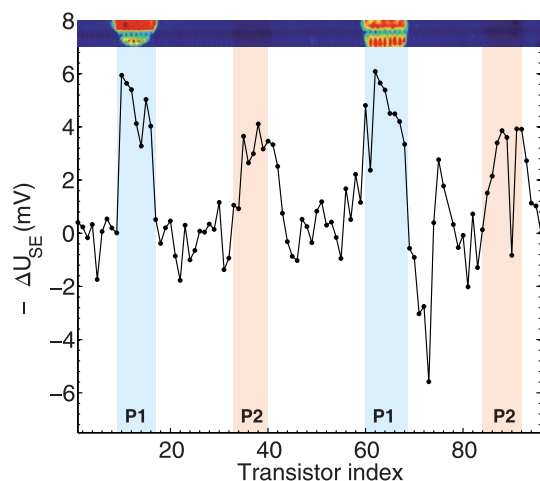


**Figure 4 | Detection of a DNA point mutation by Tas-PCR and subsequent electronic hybridization measurement.** Probes P1 have been spotted on transistors 9–17 and 60–69 and probes P2 on 33–40 and 84–92. Electronic signal (main figure) and fluorescence image (top) show that hybridization specifically occurred on probes P1. As for hybridization with oligonucleotide targets, FETs carrying hybridized probes display higher average voltage difference  $-\Delta U_{SE}$  than non-hybridized probes;  $3.9 \pm 2.0$  mV for P1 versus  $2.6 \pm 1.5$  mV for P2. Exploiting the FETs that carried no DNA, we here corrected for threshold voltage drifts between the transistors of the array<sup>14</sup>.



molecules that each exhibit a unique single stranded overhang and are otherwise entirely double-stranded. These molecules are ready for specific hybridization, no denaturation is required. In contrast, the products of standard allele-specific PCR (as-PCR) are fully double-stranded and therefore must be denatured before hybridization. Such a denaturation leads to a mixture of single-stranded and double-stranded molecules that evolves in time by re-hybridization of the complementary strands. This behaviour is susceptible to induce signal fluctuations in hybridization with surface attached probes. Moreover, it can also lead to signal fluctuations because a surface attached duplex can denature when a competing single-stranded molecule approaches, forms a free duplex that diffuses into the bulk solution and leaves the single stranded probe at the surface. The long single-stranded molecules of a denatured as-PCR sample also can cause problems by adsorption, because single-stranded DNA exhibits stronger non-specific interactions than double-stranded DNA. This point is especially important at the low salt conditions used for direct electronic detection. Finally, when as-PCR is used to generate a multitude of different fragments in a single tube for multiplexing, once denatured these molecules can cross-hybridize in many combinations, which will make reliable electronic detection difficult. The Tas-PCR avoids these problems and also simplifies the assay.

In conclusion, dedicated immobilization, blocking and hybridization procedures allow FET-based label-free detection of DNA hybridization with micro-spots. Specific hybridization induced shifts in FET threshold voltages of a few mV. Although FET-based hybridization detection with only one probe sequence may work in some cases, we find that the presented differential procedure is significantly more reliable. Presence or absence of hybridization is measured, which is adapted to the binary character of the biological information involved in genotyping applications. Duplex detection of the single nucleotide deletion 35delG has been achieved on a single patient sample, suggesting that DNA genotyping could be a first application of direct FET detection in the field of microarray-based DNA analysis. Using the presented combination of DNA amplification and electronic measurement with a set of different Tas-PCR forward primers, multiple mutations could be interrogated in a single tube and the different products carrying individual barcodes be sorted out in parallel by hybridization on the FET array. We hope that the present work will stimulate subsequent research and development towards applications of direct FET-based detection in the biological sciences.

## Methods

**Fabrication and measurement of FET arrays.** We fabricated silicon FET arrays consisting of 96 transistors arranged on a linear grating with a 20  $\mu\text{m}$  period, where each FET has an active region of  $10 \times 10 \mu\text{m}^2$  and a separate electrical drain connection. The wafer processing is described elsewhere<sup>21</sup>. Processed wafers are diced, chips are bonded to ceramic packages and plastic wells are attached to protect the wiring during subsequent liquid incubations. The drain current  $I_D$  of each FET is measured as a function of both source-drain voltage  $U_{SD}$  and a voltage  $U_{SE}$  applied between a common source contact and an Ag/AgCl reference electrode immersed in a KCl solution covering the array. The two voltages are indicated in Fig. 1 and in the schema of the recording setup presented in Figure S5 (Supplementary Information). The voltages  $U_{SE}$  of all FETs are derived, for a fixed common  $\{I_D, U_{SD}\}$  working point, by a numerical interpolation of the measured  $I_D(U_{SD}, U_{SE})$  characteristics. The measurement protocol is visualized in Figure S6 (Supplementary Information). More detailed descriptions of the experimental setup and the measurement procedures are provided in section VIII of the supplementary information<sup>14</sup> and in an earlier publication<sup>15</sup>.

**Spotting and attachment of probe DNA.** In preparation of probe attachment, the chip surface is rinsed in turn with isopropanol, ethanol and  $\text{H}_2\text{O}$  and dried with air. It is then incubated one hour in poly(L-lysine) (PLL) dilution (P8920 Sigma, 0.01% wt/vol in  $0.1 \times \text{PBS}$ , pH 7.2), rinsed in  $\text{H}_2\text{O}$  and dried with air. Micro-droplets of probe DNA solutions are deposited with a customized piezo spotter (NP2 Gesim, Germany). Humidity control (50%) and reduced surface temperature ( $13^\circ\text{C}$ ) are used, to obtain reproducible spot diameters and slow evaporation. A 100  $\mu\text{m}$  diameter spot, as shown in Fig. 1, typically contains 800 pL DNA solution (unmodified 20 mer oligonucleotides, 30  $\mu\text{M}$  in  $\text{H}_2\text{O}$ ) and covers about 5 FETs with approximately  $2 \times 10^6$  DNA molecules per  $\mu\text{m}^2$ .

We use PLL mediated attachment of DNA. This approach does not require modified oligonucleotides and avoids the harsh treatments of silane chemistry that may affect the thin oxide layer (10 nm  $\text{SiO}_2$ ) of the FET arrays' active regions. The positive background charge of the PLL coating attracts target DNA and thus allows hybridization duration well below one hour<sup>22</sup>. This point is of particular importance for field effect detection of hybridization, where temporal drift of the FET threshold voltage can make detection of reactions that last several hours challenging<sup>20</sup>.

**Blocking procedure.** For DNA detection in microarray format efficient blocking is required to avoid losing a significant fraction of target molecules by non-specific interactions with the solid substrate and the positively charged PLL layer. We studied a number of procedures, including chemical blocking with succinic anhydride or acetic anhydride and physical blocking with BSA, SDS, EDTA or DNA<sup>23,24</sup>. We observed that many of them are not compatible with FET-based hybridization detection, because they cause non-reproducible shifts of FET threshold voltages or shift the FET working point such that hybridization signals become too small to be measured reliably. We finally found a combined chemical and physical procedure that is simple and compatible with FET-based hybridization detection using micro-spots. The procedure provides efficient blocking. It consists of 30 min incubation in acetic anhydride (containing 0.1% vol of 1-methylimidazole), an intermediate  $\text{H}_2\text{O}$  rinse and 30 min incubation with DNA (20 mer oligonucleotide at a concentration of 100 nM in 25 mM KCl, with a sequence that hybridizes to none of the other sequences of the study).

**Patient sample preparation.** Genomic DNA was obtained from a patient whole blood sample (200–350  $\mu\text{L}$  in volume) using a commercial robotic workstation for extraction and purification (QUIAGEN EZ1). The automated procedure employs a reagent cartridge and contains the following successive steps, lysis of blood cells, addition of magnetic particles, DNA binding to magnetic particles, a repeated series of magnetic separation and wash steps, and finally, elution with an elution volume of 50–200  $\mu\text{L}$ .

This extracted and purified genomic DNA is used in a PCR preamplification step that selectively amplifies a DNA fragment encompassing the 35delG mutation. The protocol of this preamplification PCR and the corresponding product purification is provided in section IV of the Supplementary Information. A small amount ( $\sim 2 \times 10^{-14}$  mol) of the purified PRC preamplification product is subsequently used in the Tas-PCR. The detailed protocol of the Tas-PCR and the final product purification are given in section V of the Supplementary Information.

- Bergveld, P. Development, Operation, and Application of the Ion-Sensitive Field-Effect Transistor as a Tool for Electrophysiology. *Trans. Biomed. Eng.* **19**, 342–351 (1972).
- Fromherz, P. A neuron-silicon junction: a Retzius cell of the leech on an insulated-gate field-effect transistor. *Science* **252**, 1290–1293 (1991).
- Rothberg, J. M. *et al.* An integrated semiconductor device enabling non-optical genome sequencing. *Nature* **475**, 348–352 (2011).
- Romualdi, C., Trevisan, S., Celegata, B., Costa, G. & Lanfranchi, G. Improved detection of differentially expressed genes in microarray experiments through multiple scanning and image integration. *Nucl. Acids. Res.* **31**, e149 (2003).
- Fare, T. L. *et al.* Effects of Atmospheric Ozone on Microarray Data Quality. *Anal. Chem.* **75**, 4672–4675 (2003).
- Souteyrand, E. *et al.* Direct Detection of the Hybridization of Synthetic Homopolymer DNA Sequences by Field Effect. *J. Phys. Chem. B* **101**, 2980–2985 (1997).
- Fritz, J., Cooper, E. B., Gaudet, S., Sorger, P. K. & Manalis, S. R. Electronic detection of DNA by its intrinsic molecular charge. *Proc. Natl. Acad. Sci. USA* **99**, 14142–14146 (2002).
- Pouthas, F., Gentil, C., Côte, D. & Bockelmann, U. DNA detection on transistor arrays following mutation-specific enzymatic amplification. *Appl. Phys. Lett.* **84**, 1594–1596 (2004).
- Uslu, F. *et al.* Label-free fully electronic nucleic acid detection system based on a field-effect transistor device. *Biosens. Bioelectron.* **20**, 1723–1731 (2004).
- Hahn, J. & Lieber, C. M. Direct Ultrasensitive Electrical Detection of DNA and DNA Sequence Variations Using Nanowire Nanosensors. *Nanoletters* **4**, 51–54 (2004).
- Sakata, T. & Miyahara, Y. Potentiometric Detection of Single Nucleotide Polymorphism by Using a Genetic Field-effect transistor. *ChemBioChem* **6**, 703–710 (2005).
- Gentil, C., Philippin, G. & Bockelmann, U. Signal enhancement in electronic detection of DNA hybridization. *Phys. Rev. E* **75**, 011926 (2007).
- Sorgenfrei, S. *et al.* Label-free single-molecule detection of DNA-hybridization kinetics with a carbon nanotube field-effect transistor. *Nature Nanotech.* **6**, 126–132 (2011).
- See Supplemental Material at website.
- Pouthas, F. *et al.* Spatially resolved electronic detection of biopolymers. *Phys. Rev. E* **70**, 031906 (2004).
- Denoyelle, F. *et al.* Clinical features of the prevalent form of childhood deafness, DFNB1, due to a connexin-26 gene defect: implications for genetic counselling. *The Lancet* **353**, 1298–1303 (1999).
- Shoemaker, D. D., Lashkari, D. A., Morris, D., Mittmann, M. & Davis, R. W. Quantitative phenotypic analysis of yeast deletion mutants using a highly parallel molecular bar-coding strategy. *Nat. Genet.* **14**, 450–456 (1996).



18. Hardenbol, P. *et al.* Highly multiplexed molecular inversion probe genotyping: Over 10,000 targeted SNPs genotyped in a single tube assay. *Genome Res.* **15**, 269–275 (2005).
19. Hou, C. S. J. *et al.* Label-Free Microelectronic PCR Quantification. *Anal. Chem.* **78**, 2526–2531 (2006).
20. Perréard, C., Blin, A. & Bockelmann, U. Threshold voltage drift of FET sensor arrays with different gate insulators. *Sensors and Actuators B: Chemical* **185**, 282–286 (2013).
21. Kiessling, V., Müller, B. & Fromherz, P. Extracellular Resistance in Cell Adhesion Measured with a Transistor Probe. *Langmuir* **16**, 3517–3521 (2000).
22. Belosludtsev, Y. *et al.* Nearly Instantaneous, Cation-Independent, High Selectivity Nucleic Acid Hybridization to DNA Microarrays. *Biophys. Res. Commun.* **282**, 1263–1267 (2001).
23. Schena, M., Shalon, D., Davis, R. W. & Brown, P. O. Quantitative Monitoring of Gene Expression Patterns with a Complementary DNA Microarray. *Science* **270**, 467–470 (1995).
24. Belosludtsev, Y. *et al.* DNA Microarrays Based on Noncovalent Oligonucleotide Attachment and Hybridization in Two Dimensions. *Anal. Biochem.* **292**, 250–256 (2001).

## Acknowledgments

We are grateful to D. Feldmann (Hôpital Armand-Trousseau, Paris) for providing DNA with 35delG mutations and to M. Völker and P. Fromherz (Max Planck Institut für Biochemie, Martinsried, Germany) for cleanroom access, advice and help in the fabrication of the FET arrays.

## Author contributions

A.B. and I.C. performed experiments and data analysis. U.B. designed the research and fabricated the transistor arrays. All the authors contributed to the writing of the paper.

## Additional information

**Supplementary information** accompanies this paper at <http://www.nature.com/scientificreports>

**Competing financial interests:** The authors declare no competing financial interests.

**How to cite this article:** Blin, A., Cissé, I. & Bockelmann, U. Electronic hybridization detection in microarray format and DNA genotyping. *Sci. Rep.* **4**, 4194; DOI:10.1038/srep04194 (2014).



This work is licensed under a Creative Commons Attribution-NonCommercial-NoDerivs 3.0 Unported license. To view a copy of this license, visit <http://creativecommons.org/licenses/by-nc-nd/3.0>